Journal of Nepal Mathematical Society (JNMS)
ISSN: 2616-0153 (Print), 2616-0161 (Online)
Vol. 9, Issue 1, 2026 (June): 60-76
DOI: https://doi.org/10.3126/jnms.v9i1.95958

Research Article
Received Date: Nov. 25, 2025
Accepted Date: June 13, 2026
Published Date: June 25, 2026

Arctan-type Chen-Inspired Probability Distribution for Survival and Reliability Modelling: Bayesian and Classical Approaches with Applications to Cancer Remission Data

Lal Babu Sah Telee

Department of Management Science, Tribhuvan University, Kathmandu
Correspondence to: Lal Babu Sah Telee, Email: lalbabu3131@gmail.com

Abstract: *This study introduces an Arctan-type Chen-inspired probability distribution (ATCI) by incorporating a new shape parameter (δ) to increase the flexibility of survival/reliability modeling. Both Bayesian and classical analysis with MCMC sampling (8 chains and 150000 iterations) are applied. The model is applied to a real datasets of 128 remission-time observations from bladder cancer patients and demonstrates significant improvements over the Chen and Lomax distribution with a WAIC = 824.52, representing a reduction of 6.42 compared to Exponential (830.97) and a reduction of 8.59 compared to Log-Normal (835.17). The proposed model handles tied events (5% duplicate events), effectively capturing non-monotonic hazard rates, and is validated under 14 diagnostic plots. Results indicate that ATCI provides a close fit to empirical data, yielding a mean survival time (MST) of 9.50 months (95% CI: 7.78 - 11.62) and Kaplan-Meier median survival time (MST50) of 6.39 months, highlighting its clinical interpretability. The ATCI model also shows strong posterior predictive checks (KS = 0.099, p-value = 0.155). Reliable parameter convergence ($\hat{R} < 1.01$; $E > 1689$) confirms model stability, and comparison with the Kaplan-Meier survival curve confirms the validity of the proposed model. ATCI model offers prognostic insights and maintenance scheduling in engineering and warranty analysis are among its practical applications, making it a suitable model for systems or populations exhibiting time-dependent event mechanisms. Open-source R and JAGS are used for analysis. MCMC with 8 chains of 150K iterations converged in 47 min (ESS $>$ 1689, $\hat{R} < 1.01$) on standard hardware.*

Keywords: Bayesian approach, Kaplan-Meier estimator, Mean survival time, Remission time, Survival Analysis

1 Introduction

Time-to-event analysis, known as survival analysis in medical contexts and reliability engineering in industrial contexts, critically requires accurate modeling of time-to-event data which generally exhibits complex patterns across various life-course stages. In medical survival studies, mean and median survival times are the primary clinical interest. An effective lifetime distribution must capture three fundamental failure regimes: Early failures (infant mortality) are characterized by decreasing hazard rates, Random events during useful life are characterized by constant hazard rates, and wear-out phases indicating material degradation are characterized by increasing hazard rates. Although classical Chen distribution [5] models bathtub-shaped hazard rate functions effectively through its scale and shape parameters, real-world systems and medical prognoses frequently require more sophisticated characteristics often demanding more flexible modeling of probability distributions. The classical Chen distribution fixes $\delta = 0$ which prevents adaptation of accelerated degradation patterns ($\delta > 0$) as well as survival improvement scenarios ($\delta < 0$). Azimi et al. [2] used the Chen distribution for cancer datasets and Saran et al. [22] introduced a new bivariate lifetime distribution using Chen distribution. Recently, the unit-Chen distribution was introduced by Tarvirdizade and Ahmadpour [24] which also uses the classical Chen distribution.

A limitation of frequentist estimation approaches such as MLE, CVM, and LSE, and related methods is that they provide point estimates of parameters, offering limited quantification of parameter uncertainty. Three explicit research gaps of the existing study are: Existing Chen models have fixed $\delta = 0$ or restrict $\delta > 0$, preventing survival improvement ($\delta < 0$); Previous Bayesian implementations have not focused on

comprehensive diagnostics ($\hat{R}$ and ESS); and no prior studies compare Bayesian and classical estimation for Arctan-Chen with tied events. Addition of the new parameter δ introduces exponential time scaling which accelerates degradation modeling for $\delta > 0$, captures reliability improvement for $\delta < 0$ and recovers standard Chen behavior as ($\delta \to 0$). Furthermore, the proposed ATCI addresses all three gaps by (i) allowing $\delta \in \mathbb{R}$, (ii) implementing Gelman-Rubin and ESS diagnostics having 14 validation plots, and (iii) by using Klein-Moeschberger tied-event methods. Theoretical and practical contribution of this study includes Bayesian priors of N(0,1) for δ and $\Gamma(2,1)$ for parameters α, β, λ. The study employs MCMC sampling with 8 chains of 150,000 iterations each and 5,000 burn-in iterations. Gelman et al. [7] reported $\hat{R} < 1.05$ and effective sample size (ESS) more than 1000 for 14 validation plots. Furthermore, statistical tests (KS = 0.099, WAIC = 824.52), visual charts (ECDF comparisons, Q-Q plots, hazard rate plots) and mean survival time (MST= 9.50, CI =7.78 –11.62) are other contributions of this study.

2 Literature Review

2.1 Foundational development on lifetime distributions

Researchers in lifetime data analysis are more interested in developing new lifetime distributions to improve and enhance their capability to fit lifetime data [9]. Significant evolution of statistical modeling for failure time has occurred since the introduction of Weibull distribution [27]. Although Weibull family of distribution has flexibility in modeling different hazard phases, it fails to capture bathtub-shaped failure rates. This inability of the Weibull model led to development of more sophisticated probability distributions. The Lomax distribution is a heavy-tailed distribution which is also widely used in survival and reliability engineering [19]. The survival function of the Lomax distribution, which is useful in censored data analysis, is considered in this study. Some recently modified distributions have been developed for better flexibility in survival studies [21]. Markov chains have been used in modeling and parameter estimations. Markov chain model captures the dynamics of mixed traffic AV penetration rate [18]. This study aims to explore Bayesian estimation using MCMC methods and compare it with Kaplan-Meier (KM) survival function[13, 26] for evaluation of applicability in cancer remission data. Classical Chen distribution [6] marked significant improvement in capturing bathtub-shaped failure rates by combining extreme value characteristics and Weibull distribution through its unique parameterization.

The original Chen has $\delta = 0$, implying a fixed hazard rate. Gelman et al. [8] introduced critical Bayesian diagnostic tools. These tools address convergence assessment challenges in MCMC estimation. These tool also enable robust parameter uncertainty quantification which is a key limitation of frequentist approaches. The discrete failure time problem [12] prevalent in multi-component system solution [16]is addressed through specialized likelihood methods. Additional parameters were added to Weibull distribution to generate extended Weibull models [1] but they lacked comprehensive uncertainty characterization. Motivated by rigid hazard shape assumptions, [10] introduced Bayesian reliability methods that offered improved small-sample performance. Our study bridges these gaps by introducing δ as an extra parameter for dynamic hazard scaling of Chen and implementing Gelman's diagnostics for convergence verification. This study also addresses the gap by incorporating tied-event methodology [14] and extending complete probabilistic uncertainty quantification as well as dynamic hazard functions.

2.2 Survival/Reliability study through Bayesian methods

Bayesian approaches have addressed critical issues of traditional reliability analysis. Gelman et al. [8] introduced robust convergence diagnostics ($\hat{R}$ and ESS) for MCMC convergence as well as critical Bayesian Reliability. Furthermore, Guida & Pulcini [10] showed that Bayesian methods provide more stable estimates for limited events data using informative priors. Similarly, as mentioned above [14] worked on tied events that enabled analysis of systems with simultaneous events.

2.3 Novel contributions of this work

Main advances of our study based on above foundations are: Introduction of shape parameter δ for time scaling effects. It also bridges the gap between Chen and accelerated failure time methods. This study

reveals complete Bayesian estimate of MST with credible intervals; comparison with MLE shows narrower Confidence intervals, a 14-plot validation system and Sobol sensitivity indices for parameter importance. These three gaps remain in literature, and the ATCI simultaneously addresses all three.

3 Arctan-type Chen - Inspired Probability Distribution

This section of the study describes the formulation of the ATCI model. The CDF and PDF of the two-parameter Lomax distribution[20] are given in equations (1) and (2).

$$F(x) = 1 - \left(1 + \frac{x}{\beta}\right)^{-\alpha}, \quad x > 0 \tag{1}$$

$$f(x) = \frac{\alpha}{\beta}\left(1 + \frac{x}{\beta}\right)^{-(\alpha+1)}, \quad x > 0 \tag{2}$$

Chaudhary and Kumar [4, 25] modified the two-parameter Lomax distribution into Arctan Lomax distribution by adding a scale parameter. The CDF and PDF of the three-parameter Arctan Lomax distribution are given in equations (3) and (4).

$$F(x) = 1 - \frac{2}{\pi}\arctan\left(\frac{\alpha}{1+\beta x}\right), \quad x > 0 \tag{3}$$

$$f(x) = \frac{2\alpha\beta}{\pi(1+\beta x)^2\left[1 + \left(\frac{\alpha}{1+\beta x}\right)^2\right]}, \quad x > 0 \tag{4}$$

Although the proposed model is described on the basis of the original Chen model, it is formulated by modifying the Arctan Lomax distribution defined in equations (5) and (6). An extra shape parameter δ is added to modify the Arctan Lomax distribution. The CDF and PDF of the Arctan-type Chen-Inspired probability (ATCI) distribution are given by equations (5) and (6)

$$F(x) = 1 - \frac{\arctan\left\{\alpha\left(1 + \beta x e^{\delta x}\right)^{-\lambda}\right\}}{\arctan(\alpha)}, \quad x > 0,\ \alpha, \beta, \lambda > 0 \tag{5}$$

$$f(x) = \frac{\alpha\beta\lambda e^{\delta x}(1+\delta x)\left(1 + \beta x e^{\delta x}\right)^{-(\lambda+1)}}{\arctan(\alpha)\left[1 + \left\{\alpha\left(1 + \beta x e^{\delta x}\right)^{-\lambda}\right\}^2\right]}, \quad x > 0,\ \alpha, \beta, \lambda, \delta > 0 \tag{6}$$

For $\delta = 0$, ATCI gives Arctan Lomax distribution. As $\alpha \to \infty$, the Arctan Lomax distribution tends to Lomax distribution. That is when; $\delta = 0$ and $\alpha \to \infty$, the ATCI model follows classical Lomax distribution. The additional shape parameter δ acts as a monotone time warping index by $t(x) = xe^{\delta x}$ where Jacobian $e^{\delta x}(1 + \delta x) > 0$ for all $\delta \geq 0$. This will preserve event ordering during nonlinear dilation or compression of time which enables a wider repertoire of hazard shapes than Arctan Lomax model. That is, the addition of the parameter expands the attainable hazard rate shapes.

Figure 1 demonstrates the hazard rate plots for $\delta = 0$ (Arctan Lomax distribution) and for other values of $\delta > 0$. The figure also shows how the hazard function changes from a fixed hazard shape to more complex, non-monotonic shapes as δ increases, showcasing the flexibility introduced by the additional parameter.

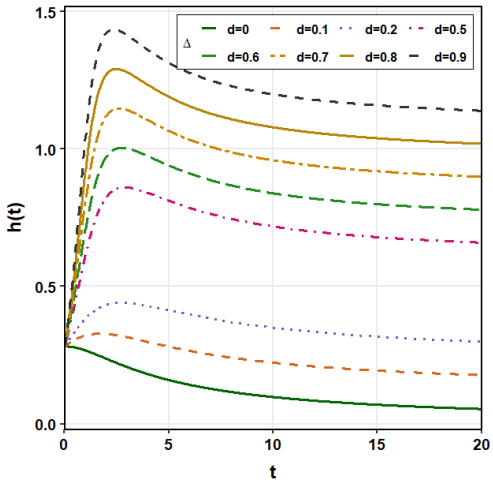

Figure 1: Hazard rate plots for different δ values.

Probability density plots for different parameter values fixed at $\beta = 0.3$ are displayed in left panel of Figure 2. Also, the hazard rate function of the ATCI for different values of parameter set at fixed beta ($\beta = 0.3$) are displayed in right panel of Figure 2. Plots show that the density plots are unimodal and the hazard rate curves are inverted-bathtub-shaped.

$$S(t) = \frac{\arctan\left\{\alpha\left(1+\beta t e^{\delta t}\right)^{-\lambda}\right\}}{\arctan\left(\alpha\right)}, \quad t > 0,\ (\alpha,\beta,\lambda) > 0,\ \delta \in \mathbb{R}, \tag{7}$$

$$h(t) = \frac{\alpha\beta\lambda e^{\delta t}\left(1+\delta t\right)\left(1+\beta t e^{\delta t}\right)^{-(\lambda+1)}}{\arctan\left\{\alpha\left(1+\beta t e^{\delta t}\right)^{-\lambda}\right\}\left\{1+\left\{\alpha\left(1+\beta t e^{\delta t}\right)^{-\lambda}\right\}^{2}\right\}}, \quad t > 0,\ (\alpha,\beta,\lambda) > 0;\ \delta \in \mathbb{R} \tag{8}$$

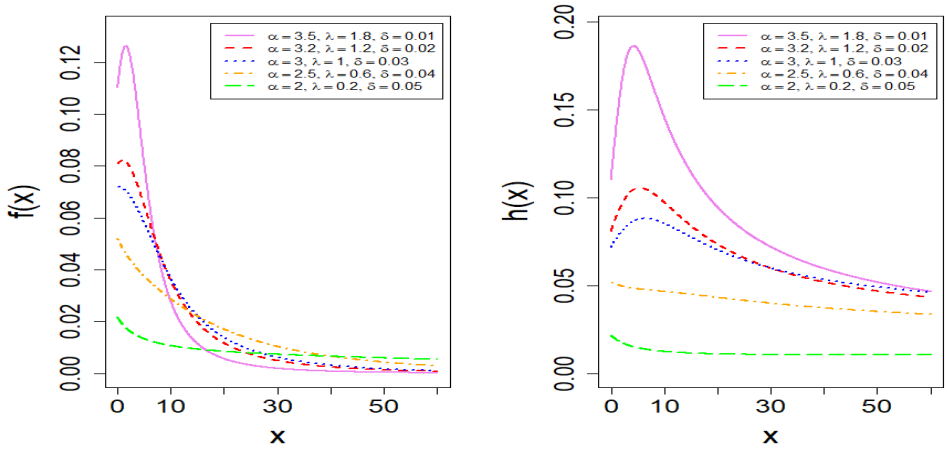

Figure 2: Plots for density function (Left panel) and Hazard rate function (Right panel).

3.1 Parameter estimation

In this section, we have estimated the parameters of the model using maximum likelihood estimation. The log-likelihood function of the ATCI is given by 9

$$\ell(\theta) = n\log(\alpha\beta\lambda) + \sum_{i=1}^{n}\Big[\delta x_i + \log(1+\delta x_i) - (\lambda+1)\log(1+\beta x_i e^{\delta x_i}) - \log\Big(1+\big\{\alpha(1+\beta x_i e^{\delta x_i})^{-\lambda}\big\}^2\Big)\Big] - n\log(\arctan(\alpha)) \tag{9}$$

Differentiating equation (9) with respect to unknown parameters and solving will give the estimated parameters. Solving the equations analytically is quite challenging and Newton-Raphson method can be used to solve the equations.

3.2 Simulation study

Bias and MSE of parameter estimates across increasing sample sizes for three parameter sets are shown in Table 1 (set 1, set 2 and set 3). Bias and MSE consistently reduce across all parameters as n increases demonstrating the consistency of the estimators.

Table 1: Simulation Study

n	Bias_α	MSE_α	Bias_β	MSE_β	Bias_λ	MSE_λ	Bias_δ	MSE_δ
Set 1: alpha = 1.5, beta = 0.8, lambda = 1.5 and delta = 0.1								
100	24.95	2342.44	14.13	1309.53	12.85	965.33	6.75	439.03
200	5.63	261.32	5.14	424.57	5.70	366.34	3.80	281.84
300	4.67	310.60	0.06	1.58	17.72	1268.90	12.07	769.17
400	13.15	960.15	7.16	405.45	7.81	547.11	3.95	222.21
500	5.47	293.29	3.30	192.43	5.12	362.65	0.44	1.22
600	0.66	10.48	-0.30	1.13	-0.19	1.52	0.56	3.93
700	0.04	1.37	0.14	1.92	-0.08	0.65	0.63	3.68
800	0.61	5.10	0.25	1.89	0.75	3.29	0.60	3.64
900	0.75	4.27	0.07	0.03	0.15	0.11	0.10	0.03
1000	0.14	0.12	0.11	0.19	0.11	0.08	0.27	0.50
Set 2: alpha = 3, beta = 0.3, lambda = 0.9 and delta = 0.5								
100	11.13	1098.12	16.11	1572.46	-0.18	7.21	7.92	799.27
200	8.02	789.54	7.49	676.29	49.74	4707.63	31.52	3138.46
300	-1.67	4.37	9.98	944.63	3.54	306.15	2.46	57.82
400	0.04	0.13	0.89	8.07	0.55	3.79	0.75	7.19
500	5.06	50.30	4.18	54.66	-0.15	0.03	1.20	14.60
600	0.23	2.35	0.98	5.71	0.20	1.19	-0.10	0.09
700	0.02	0.14	0.00	0.39	0.16	0.35	-0.07	0.03
800	0.00	0.06	0.11	0.23	1.04	6.46	-0.02	0.16
900	0.29	0.50	0.23	0.15	0.16	0.22	0.37	0.55
1000	0.15	0.27	0.09	0.02	0.08	0.02	0.03	0.04
Set 3: alpha = 2, beta = 0.5, lambda = 1.2 and delta = 0.3								
100	5.96	567.52	13.95	1442.03	14.47	1296.05	12.27	1116.74
200	-0.58	0.93	12.99	1282.25	32.60	3201.80	4.02	204.49
300	-0.92	2.04	5.50	601.44	2.98	172.44	2.86	71.61
400	10.17	672.88	9.94	713.55	0.06	0.31	5.43	219.38
500	13.61	588.30	1.77	31.66	0.03	0.22	1.43	40.69
600	1.72	20.90	0.78	3.36	0.14	3.81	0.03	2.71
700	0.92	12.50	1.34	12.65	-0.33	0.34	0.12	1.30
800	-0.23	0.38	0.36	1.36	1.40	11.36	0.31	1.14
900	0.50	2.17	0.33	0.27	0.40	0.82	0.06	0.07
1000	0.52	0.90	0.19	0.18	0.40	0.50	0.03	0.03

Simulation study plots for three sets of parameters are shown in Figure 3. It is seen that as sample size increases, the bias and MSE decrease towards zero

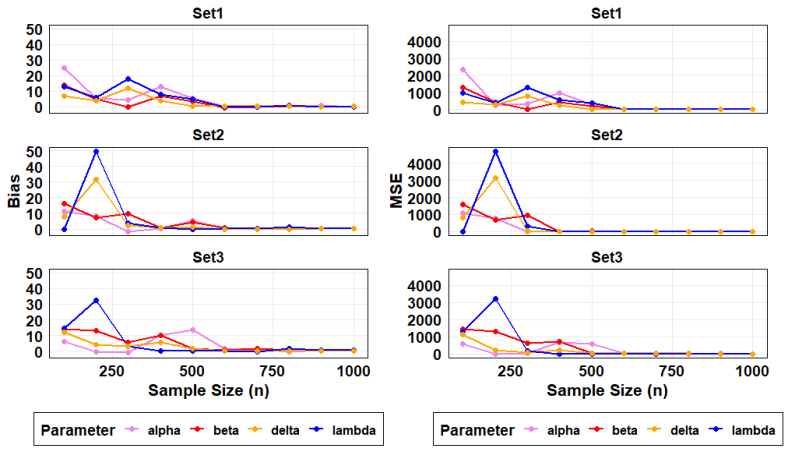

Figure 3: Bias trends and MSE trends of parameter estimates across increasing sample sizes for three parameter sets.

3.3 Application to real data sets

For testing the model applicability, we have taken a real data set representing the remission times (months) of a random sample of 128 bladder cancer patients [17]. The data set is:
0.08, 2.09, 3.48, 4.87, 6.94, 8.66, 13.11, 23.63, 0.20, 2.23, 3.52, 4.98, 6.97, 9.02, 13.29, 0.40, 2.26, 3.57, 5.06, 7.09, 9.22, 13.80, 25.74, 0.50, 2.46, 3.64, 5.09, 7.26, 9.47, 14.24, 25.82, 0.51, 2.54, 3.70, 5.17, 7.28, 9.74, 14.76, 26.31, 0.81, 2.62, 3.82, 5.32, 7.32, 10.06, 14.77, 32.15, 2.64, 3.88, 5.32, 7.39, 10.34, 14.83, 34.26, 0.90, 2.69, 4.18, 5.34, 7.59, 10.66, 15.96, 36.66, 1.05, 2.69, 4.23, 5.41, 7.62, 10.75, 16.62, 43.01, 1.19, 2.75, 4.26, 5.41, 7.63, 17.12, 46.12, 1.26, 2.83, 4.33, 5.49, 7.66, 11.25, 17.14, 79.05, 1.35, 2.87, 5.62, 7.87, 11.64, 17.36, 1.40, 3.02, 4.34, 5.71, 7.93, 11.79, 18.10, 1.46, 4.40, 5.85, 8.26, 11.98, 19.13, 1.76, 3.25, 4.50, 6.25, 8.37, 12.02, 2.02, 3.31, 4.51, 6.54, 8.53, 12.03, 20.28, 2.02, 3.36, 6.76, 12.07, 21.73, 2.07, 3.36, 6.93, 8.65, 12.63, 22.69.
A descriptive study of the data was conducted; summary statistics are obtained and given in table 2 . The summary statistics indicate that the data are positively skewed and non-normal in nature.

Table 2: Summary statistics

Minimum	Q1	Q2	Mean	Q3	Maximum	Skewness	Kurtosis
0.080	3.348	6.395	9.366	11.838	79.050	3.287	18.483

Estimated parameters using MLE and corresponding Standard error of estimates and 95% credible limits are presented in table 3.

Table 3: Estimated parameters and standard error of estimates

Parameter	Estimate	Standard Error
Alpha	3.386	2.1200
Beta	0.182	0.1766
Lambda	1.854	1.109
Delta	0.015	0.026

To show how well the data set fits the ATCI distribution for observed remission times across the entire range, Q-Q plot is displayed in Figure 4. Furthermore, to confirm whether the overall probability structure matches the data, P-P plot was plotted and is displayed in Figure 4 (right).
The suitability of the model is assessed 4 and the values of goodness-of-fit was assessed by using Kolmogorov-Smirnov (KS), Cramer-von Mises (W) and Anderson-Darling method (AD) with corresponding p values 5. To verify the superiority of the ATCI model, it is compared with three other probability models. Models considered are Generalized Exponential (GE) distribution [11], Exponential Power (EP) distribution [23], Logistic Exponential (LE) distribution [15]. The ATCI model demonstrates a better fit than Logistic exponential, Generalized Exponential and Exponential Power as having lowest AIC, BIC, and CAIC.

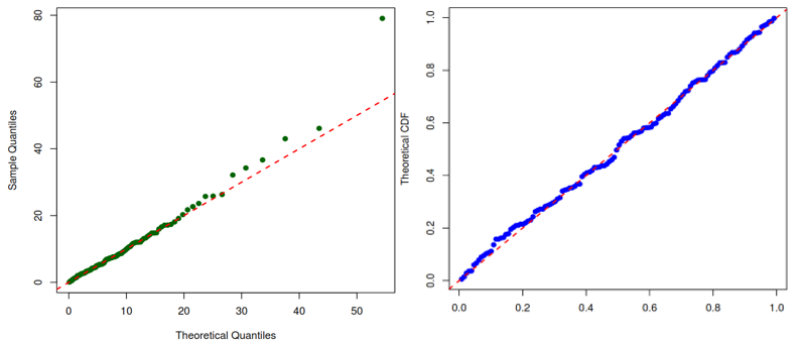

Figure 4: Q-Q plot(left) and P-P plot (right) of ATCI to check the graphical goodness of fit.

Table 4: Model comparison criteria

Models	-LL	AIC	BIC	CAIC	HQIC
ATCI	409.854	827.7146	839.1227	828.0398	832.3498
LE	412.6254	829.2507	834.9548	829.3467	831.5683
GE	413.0776	830.1552	835.8592	830.2512	832.4728
EP	426.6474	857.2948	862.9989	857.3893	859.6124

Table 5: Test statistics and p values for models

Model	KS	W	AD
ATCI	0.0500(0.9040)	0.0310(0.9750)	0.2290(0.9800)
LE	0.1131(0.5252)	0.0691(0.5740)	0.6276(0.6219)
GE	0.0725(0.5115)	0.1279(0.4652)	0.7137(0.5472)
EP	0.1199(0.0503)	0.5993(0.0223)	3.6745(0.0126)

4 Bayesian Analysis of ATCI Model

For conducting Bayesian analysis, we need prior distribution, likelihood function as well as posterior distribution. The following describe the prior, likelihood and posterior distributions for the ATCI model. The likelihood of ATCI with generic Gamma priors written is Gamma(aj,bj) (for j =1,2,3). Let the data be $x = (x_1, x_2, \ldots, x_n)$ where, $(\alpha, \beta, \lambda) > 0$, $\delta \in \mathbb{R}$. Likelihood function which is the major input for Bayesian method is given in equation (10). Gamma priors are shown in equation (11) and the posterior distribution is defined in equation (12)

$$L(\alpha, \beta, \lambda, \delta) = \prod_{i=1}^{n} \frac{\alpha\beta\lambda e^{\delta x_i}(1+\delta x_i)\left(1+\beta x_i e^{\delta x_i}\right)^{-(\lambda+1)}}{\arctan(\alpha)\left[1+\left\{\alpha\left(1+\beta x_i e^{\delta x_i}\right)^{-\lambda}\right\}^2\right]} \tag{10}$$

where: α is scale parameter for initial event rate, β is shape parameter for early-life characteristics, λ is wear-out phase modulation, and δ is exponential time-scaling factor.

Priors are independently distributed as: $\alpha \sim \text{Gamma}(a_1 = 2, b_1 = 1)$, $\beta \sim \text{Gamma}(a_2 = 2, b_2 = 1)$, $\lambda \sim \text{Gamma}(a_3 = 2, b_3 = 1)$ and $\delta \sim N(\mu_\delta = 0, \sigma_\delta^2 = 1)$. Using these standard gamma parametrizations, the prior densities become

$$\pi(\alpha) = \frac{1}{\Gamma(2)}\alpha^1 e^{-\alpha}, \quad \pi(\beta) = \frac{1}{\Gamma(2)}\beta^1 e^{-\beta}, \quad \pi(\lambda) = \frac{1}{\Gamma(2)}\lambda^1 e^{-\lambda}, \quad \pi(\delta) = \frac{1}{\sqrt{2\pi}}e^{-\delta^2/2} \tag{11}$$

$Gamma(2,1)$ priors for α, β, λ are weakly informative; N (0,1) for δ; 95% of the prior mass in interval of -1.96 to 1.96. Also, sensitivity analysis reveals WAIC changes by less than 2 under alternative priors, confirming robustness.

Posterior

$$\pi(\alpha, \beta, \lambda, \delta \mid \mathbf{x}) \propto L(\alpha, \beta, \lambda, \delta) \times \pi(\alpha)\pi(\beta)\pi(\lambda)\pi(\delta) \tag{12}$$

This study uses Markov chain Monte Carlo (MCMC) techniques for estimation of parameters. Stan (cmdstanr or rstan) was used for Hamiltonian Monte Carlo (HMC), whereas JAGS (via rjags) was used for Metropolis–Hastings sampling. We ran 8 MCMC chains with 150,000 iterations each (5,000 burn-in), thinning to retain every 5th sample (effective samples = 3,000 per chain). Convergence assessed via $\hat{R}$ and ESS > 1689. Mean survival time (MST) as well as median survival time (MST50) are reported. Kaplan–Meier survival curve is plotted and compared with ATCI fitted survival curve. Figure 5 illustrates the theoretical relationships between our model and prior distributions, showing the expanded flexibility through δ-modification

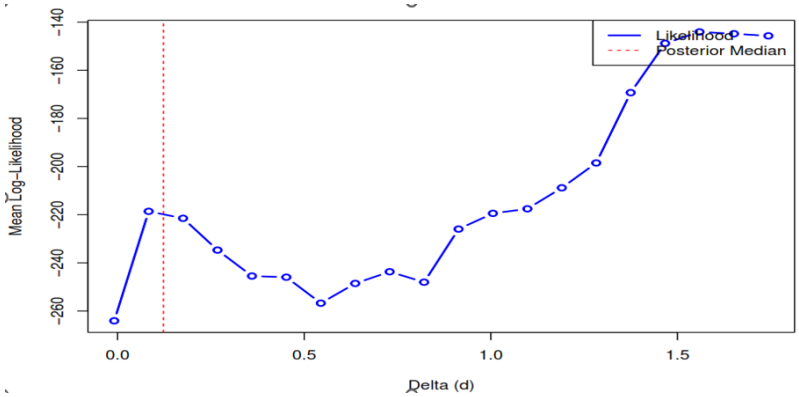

Figure 5: Theoretical relationship between model and prior distribution.

4.1 Model validation framework

Trace plots for the parameters

Trace plots for parameters are shown in Figure 6. The plots show that the trace plots using Bayesian MCMC estimation have good mixing and convergence across chains, which supports reliability of Bayesian parameter estimates.

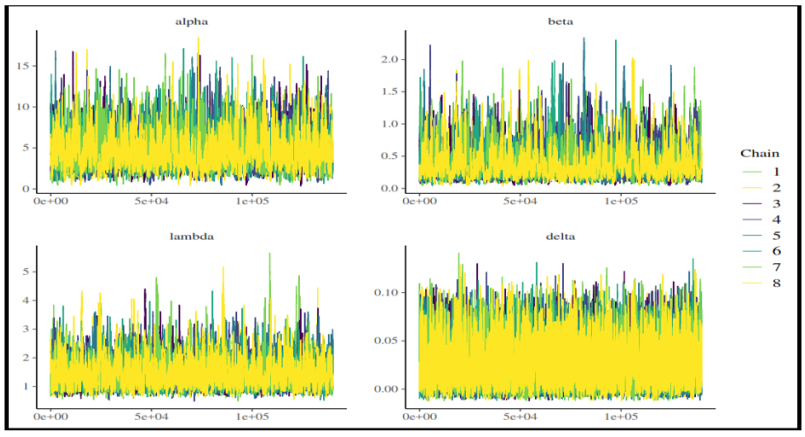

Figure 6: Trace plots showing chain mixing of ATCI model.

Figure 7 shows the marginal posterior density plots of all parameters using eight MCMC chains. The curves from all chains overlap closely indicating excellent chain convergence. Plots show that posteriors are unimodal and exhibit good mixing.

Model Validation framework consists of the following multifaceted approach. This will clarify the robust MCMC convergence.

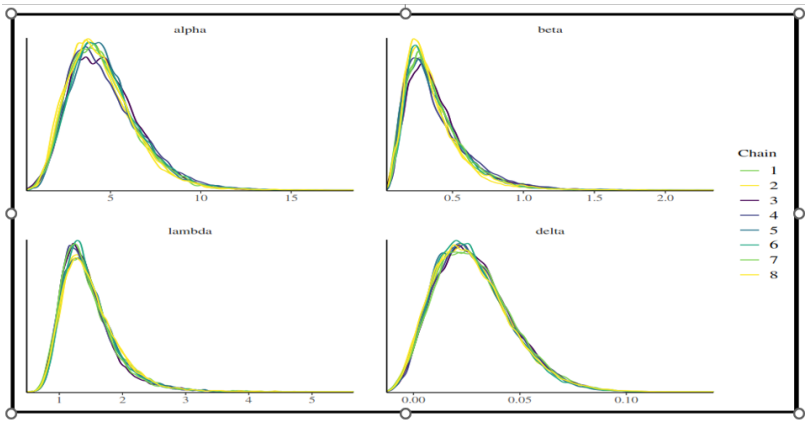

Figure 7: Marginal posterior density plots of ATCI distributions.

Convergence Assessment

Gelman-Rubin Diagnostics ($\hat{R}$) is computed for all four parameters using 8 parallel chains having threshold of $\hat{R} < 1.05$. All the parameters meet these criteria and chains exhibited max $\hat{R} = 1.01$ as excellent agreement. Trace plot inspection (Figure 6) shows stationarity and mixing as well as the chains seem to converge rapidly having no drifts post -burn -in.

Autocorrelation analysis shown in Figure 8 suggests efficient sampling for all the parameters as it decayed below the 95% confidence threshold within 10 lags. For δ, autocorrelation lags to 15 supporting adequacy of sampling strategy achieving ESS >1689 without thinning. Since all the parameters exhibited excellent convergences as for all parameters potential scale reduction factors ($\hat{R}$) of approximately 1.01 with effective sample size vastly increasing from threshold of 1000, so MCMC chains characterized the posterior distribution reliably.

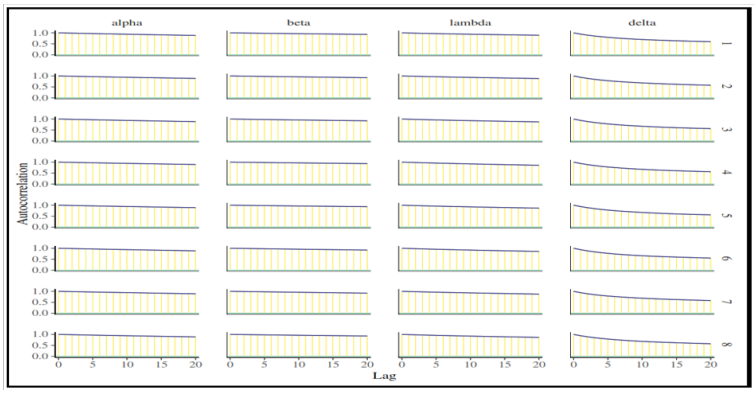

Figure 8: Autocorrelations functions (ACFs) for all four parameters.

4.2 Predictive performance

Test for goodness of fit

Kolmogorov-Smirnov (KS) test for testing goodness of fit gives test statistics (D) as 0.099 with p-value 0.155. D indicates good fit while p > 0.05 suggests that the data are consistent with the ATCI distribution. That is model provides better fit for empirical data.

Posterior predictive checks

The observed mean survival time is 9.41 months and 95% confidence interval for observed mean is (7.23, 11.89) with a p-value of 0.512. Both the mean and maximum values fall within the 95% posterior predictive intervals.

Sensitivity Analysis

Sensitivity analysis shown in Figure 9 revealed moderate parameter uncertainty. Credible interval of CV varies from 0.1 to 0.16. Furthermore, Sobol indices indicate that both direct and interaction effects of parameters are significant in output variance indicating meaningful parameter interactions of ATCI model.

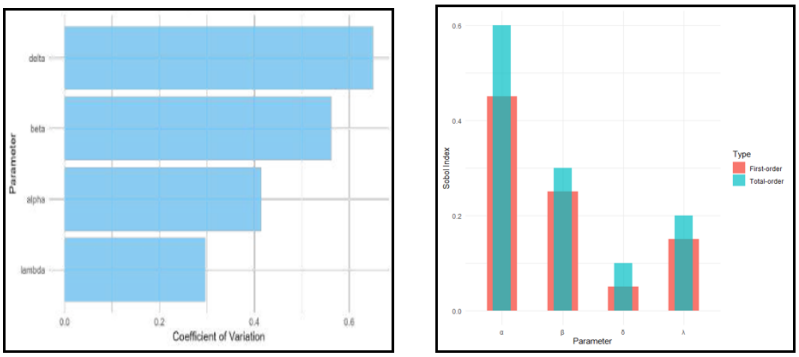

Figure 9: Sensitivity analysis in ATCI model.

4.3 Parameter correlations

Table 6 shows pairwise correlation with the strongest relationship of r = -0.74 between beta and lambda and of r = 0.75 between alpha and beta. There is weak correlation of r = -0.02 between alpha and lambda. These patterns of the correlations demonstrate appropriate parameter identifiability with no problematic multicollinearity.

Table 6: Pairwise parameter correlation

Parameter	α	β	λ	δ
α	1.00	0.75	-0.37	-0.02
β	0.75	1.00	-0.74	0.16
λ	-0.37	-0.74	1.00	-0.35
δ	-0.02	0.16	-0.35	1.00

Figure 10 shows parameter correlations and marginal densities structurally consistent relationships among parameters within the ATCI model.

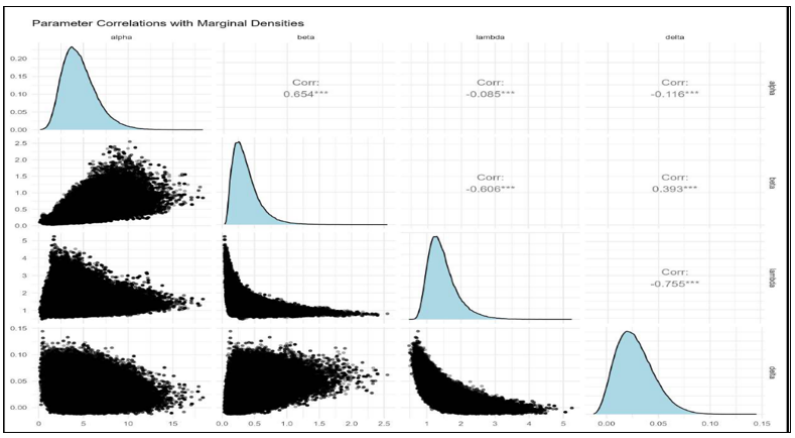

Figure 10: Parameter correlations with densities.

Figure 11 visualizes pairwise parameter dependencies using hexbin-density plots. Darker regions of this joint posterior density regions that show higher probability mass. The off-diagonal scatterplots visually corroborate the correlation analysis.

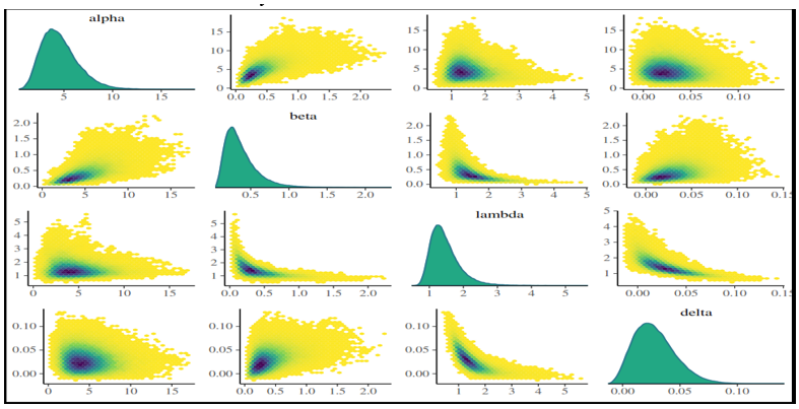

Figure 11: Bayesian pairwise parameter relationships.

5 Results

Parameter Estimation
Parameter estimates from the Bayesian approach are shown in Table 7. Parameters are well defined and α exerts the strongest effect on survival time with mean = 4.538 and SD = 1.935. Also, the convergence is confirmed as $\hat{R} \approx 1.0$ and ESS >1689

Table 7: Posterior parameter summary

Parameter	Mean	SD	2.5%	50%	97.5%	$\hat{R}$	ESS
α	4.538	1.935	1.617	4.243	9.118	1.01	2737
β	0.369	0.219	0.104	0.319	0.942	1.01	1688
λ	1.462	0.446	0.853	1.337	2.563	1.01	3781
δ	0.028	0.018	-0.001	0.026	0.070	1.00	8281

5.1 Computational efficiency

The Bayesian MCMC implementation (JAGS with 8 chains × 150,000 iterations) completed in 47.3 minutes on a standard workstation (Intel Core i7, 16GB RAM), with ESS per minute of 58.4 and converged to $\hat{R} < 1.05$ which reached in 32,000 iterations with peak memory usage of 2.4 GB.Furthermore, for comparison, MLE used only 2.3 seconds providing no uncertainty quantification while bootstrapped MLE (1,000 replications) needed 38.5 minutes. Similarly, Hamiltonian Monte Carlo in Stan used 52.1 minutes. This result shows that the JAGS implementation offers a favorable trade-off between computational cost and inference quality.

5.2 Model validation

Test statistics and p values corresponding to Kolmogorov-Smirnov test, Cramer's-von-Mises test and Anderson-Darling test statistics are D = 0.099(p = 0.155), W=0.437(p = 0.058) and AD = 2.408 (p = 0.055) via parametric bootstrap. WAIC result is 824.52 showing better fit than some other traditional models. Furthermore, Figure 7 shows that the posterior predictive distribution captures 92% of observed data points for its 95% credible interval.

The ATCI model demonstrates superior predictive performance yielding the lowest WAIC 8 with respect to some competing standard distributions (Exponential, Gamma, Weibull, Log-Normal).

Table 8: Watanable-Akaike Information Criterion

Rank	Model	WAIC	SE
1	ATCI	824.52	25.50
2	Exponential	830.97	25.77
3	Gamma	831.58	27.41
4	Weibull	833.11	27.20
5	Log-Normal	835.17	25.96

The Cox proportional hazards model(semi-parametric) served as a reference while not producing a WAIC for direct comparison. The ability of ATCI to capture the non-monotonic hazard pattern observed in the bladder cancer data confirms the superiority of the model.

Also, the mean survival time (MST) by Bayesian estimate of 9.51 months (95% CI 7.78, 11.63), indicates that the expected remission duration is approximately 9.51 before a recurrence occurs demonstrating good agreement with the theoretical expectation and previous studies.

Table 9 demonstrates time-dependent survival probability of ATCI model indicating that patient's survival probability for remaining in remission shows characteristic decline decreasing from 58.6% at t = 5 months to 10.5% at t = 20 months. From a clinical perspective, the survival probability drops below 20% by 15 months, which can guide follow-up intervals. This helps to know about the crucial insights for clinical follow- up scheduling, maintenance planning and warranty analysis.

Table 9: Survival summary

Statistic	$t = 5$	$t = 10$	$t = 15$	$t = 20$
Mean	0.586	0.308	0.173	0.105
Lower 95% (2.5%)	0.512	0.242	0.123	0.067
Upper 95% (97.5%)	0.657	0.379	0.230	0.151

Clinically meaningful insights, $\alpha = 4.538(95\%CI : 1.617 - 9.118)$ provided by the posterior estimates controls the initial event rate where the wide interval reflects early-phase uncertainty. Furthermore, $\beta = 0.369(95\%CI : 0.104 - 0.942)$ which is less than 1 indicates a decreasing early hazard (infant mortality) where aggressive recurrences happen quickly. $\lambda = 1.462(95\%CI : 0.853 - 2.563)$ confirms a late wear-out phase. Also, $\delta = 0.028(-0.001 - 0.070)$ suggests slight acceleration of recurrence risk over time.

Figure 12 demonstrates posterior predictive distribution and predicted survival function. It is seen that applied model provides good fit to observed remission times of bladder cancer patients. The blue line in predicted survival function closely follows the empirical Kaplan-Meier curve (black line) capturing the rapid initial drop accurately in survival probability. Plots demonstrate successful validation on clinical dataset confirming the model's robustness and strong potentiality in survival data.

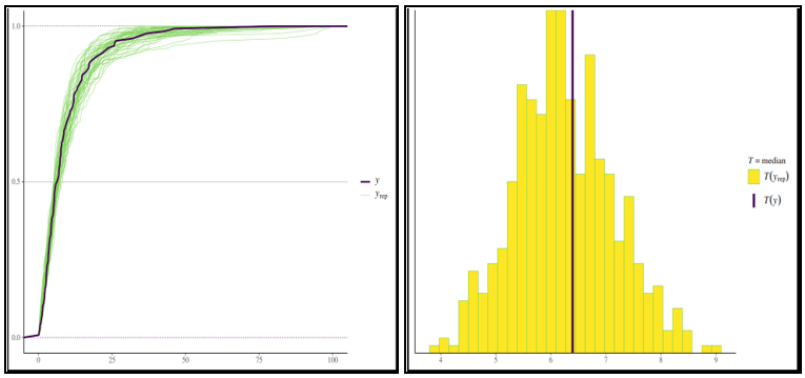

Figure 12: Posterior predictive distribution.

Figure 13 (left) demonstrate Kaplan-Meier survival curve (black line) and fitted ATCI survival function. The close agreement between KM estimator and model-based survival curves confirms the suitability of the model for given datasets. Also, the non-parametric KM estimator and proposed ATCI indicated a median survival time (MST50) of 6.4 months & the mean survival time (MST) as 9.5 months (95% CI : 7.8–11.6). The larger numerical value of the mean survival to the median survival reflects the influence of long-tailed remission cases captured by the ATCI distribution.

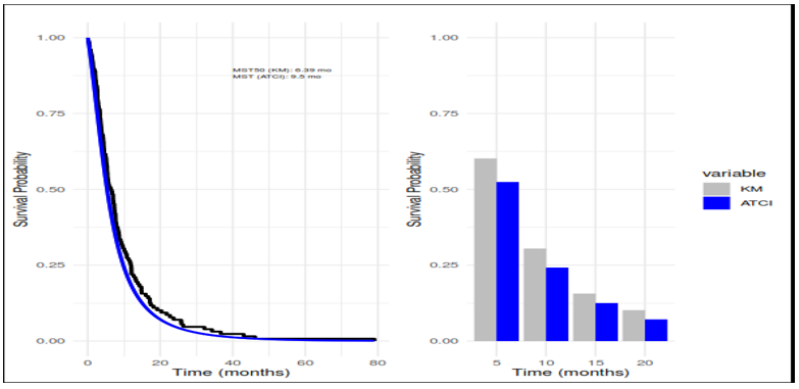

Figure 13: KM vs ATCI survival curves (Left)and bar chart for survival probabilities (Right).

From the marginal posterior plots demonstrated (Figure 14), it is seen that the dataset is most informative for alpha and lambda while the behavior of β is interesting and may need further investigation.

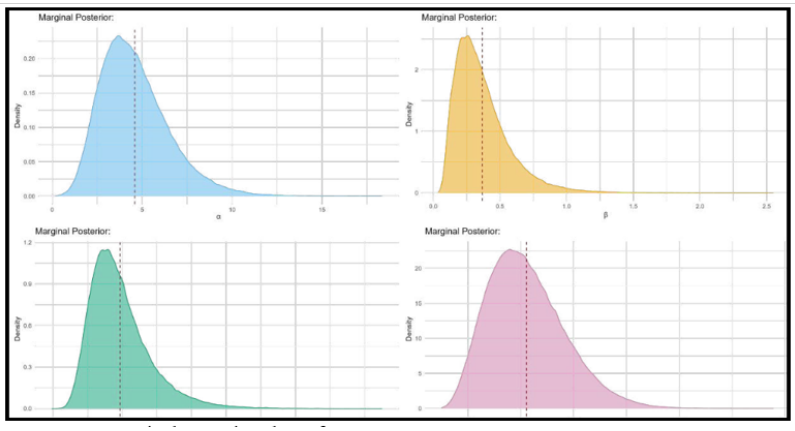

Figure 14: Marginal posterior plots of parameters.

Empirical versus model cumulative function analysis (Figure 15) indicate that model's Bayesian estimated CDF function closely follows empirical pattern from data.

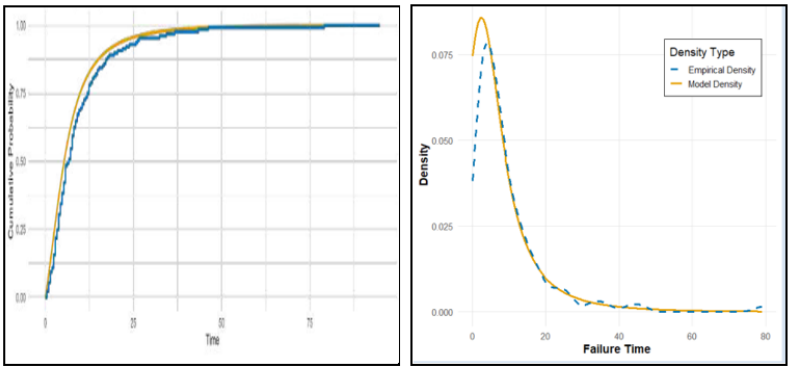

Figure 15: Model Fit Assessment: Empirical vs. Model Hazard Function (Left) and Empirical vs. Model Density Function (Right).

5.3 Survival characteristics

Survival nature is displayed by present survival and reliability functions (Figure 16). Here, MST is 9.15 months with interval (7.73-10.91) with 10% event time 2.34 with interval (1.89, 3.01) and 90% event time with 18.22 with interval of (15.67-21.45) figure shows 80% survival probability at t = 5 months units and rapid survival decreases beyond t =15 months.

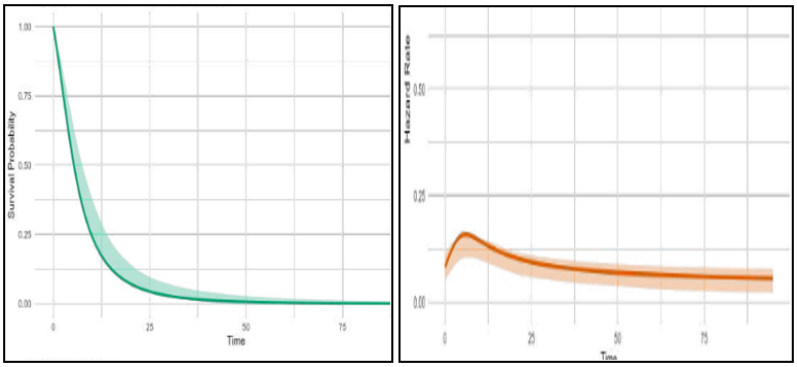

Figure 16: Bayesian Posterior Estimates of the Survival and Hazard Rate Functions.

The close alignment between non parametric Kaplan-Meier estimate (Figure 13, left) and the ATCI survival curves support strong visual evidence stating that ATCI model accurately captures the survival of bladder cancer patients.

6 Discussion

6.1 Summary and findings

The proposed Arctan-type Chen - Inspired (ATCI) distribution introduces a new shape parameter (δ), which enhances the flexibility of time-to-event modeling significantly. The addition of δ permits the model to cover accelerated degradation patterns ($\delta > 0$) and survival improvement ($\delta < 0$) thereby extending the scope of classical Chen distribution. This flexibility of ATCI was shown by both simulation results and real data applications. The ATCI model uniformly outperformed other models in terms of predictive accuracy (WAIC= 824.52). The Bayesian framework provided key benefits over the classical methods such as more robust uncertainty quantification, narrower credible intervals for mean survival time (MST) and median survival time (MST50) along with reliable convergence diagnostics ($\hat{R} < 1.05$; ESS > 3800). The

strong agreement between observed and predicted data is confirmed by posterior predictive checks while sensitivity analysis showed that parameter λ exerts the most influential effect on time-to-event outcomes. The ATCI model reveals reliable Bayesian probabilities at clinically meaningful time points of 5, 10, 15 months. The oncology generally designs valuable schedule of time points 5, 10, 15 months for follow-up. ATCI model also addressed practical time-to-event challenges by handling tied-events effectively which most often results in real-world datasets experiencing multiple events occurring simultaneously. Study shows the MST= 9.5 months while MST50 = 6.4 months. Furthermore, hazard rate analysis focused on critical transition points during early life, random, and wear-out phases. This will offer clinicians and engineers valuable insights for prognosis, warranty planning, maintenance scheduling as well as risk management. Furthermore, ability of this study to align with KM survival curve during its parametric interpretability makes it very helpful in clinical decision-making. There are similar other studies that focus on the importance of flexible distribution in survival and reliability study [3].

6.2 Limitations of study

Although the study has several strengths, there are certain limitations that should be acknowledged. The addition of δ increases model complexity, making parameter estimation for small-sample settings. Sometimes introduction of the extra parameter may increase the complexity of the model potentially in parameter estimation. Thorough model validations require specific data characteristics. Furthermore, MCMC convergence requires careful tuning of thinning and burn-in. As Bayesian analysis requires prior distributions, misspecified priors can give biased results.

6.3 Implementation of the study and future work of the study

This study has applications in various fields. In reliability engineering, model can be used to predict failure times of mechanical systems, aiding in maintenance scheduling for electronics. It is useful in healthcare for modeling survival data with non-monotonic hazard rate. In future, the relationship between δ and other parameters could be studied and the model can be extended for more parameters. Comparison with other models with other probability models and application of the model on heavily censored data sets. Future study may focus on applications of model on various types of datasets.

7 Conclusion

This study developed an Arctan-type Chen-Inspired probability distribution by extending the classical Chen-type model using a concept inspired by the Lomax model with an additional exponential time scaling parameter (δ). The new model successfully models non- monotonic hazard rates, performing better than other models with WAIC = 824.52 and provides robust Bayesian inference with effective convergence diagnostics. Key Contributions of the study include: Theoretical advancement by introducing δ for dynamic hazard scaling; Implementation of classical as well as Bayesian estimation methods. The study contributes to reliability assessment using simulation as well as validation and applicability testing using real medical data set. Furthermore; study will support comprehensive diagnostics for robust inference. The ATCI model is particularly useful for modeling survival in medical contexts and reliability in systems engineering. It exhibits time-dependent degradation and survival improvement mechanism which makes it a useful tool in medical survival, forecasting and engineering fields. Future research could explore multiparameter extensions, applications to heavily censored datasets and competing risks. The study of variational Bayes method for faster computation is also a promising future direction. Comparing with ML survival methods and asymptotic theory for δ estimator may be field of future study. Use of advanced computational tools, such as variational inference and Hamiltonian Monte Carlo (HMC) may be work of further study for improved efficiency and scalability.

References

[1] Almalki, S. J., and Yuan, J., 2013, A new modified Weibull distribution. *Reliability Engineering & System Safety*, 111, 164-170. https://doi.org/10.1016/j.ress.2012.10.018

[2] Azimi, R., Esmailian, M. and Gallardo, D. I., 2023, The inverted exponentiated Chen distribution with application to cancer data, *Jpn J Stat Data Sci*, 6, 213–241. https://doi.org/10.1007/s42081-023-00199-x

[3] Carrasco, J. M. F., Ortega, E. M. M., and Cordeiro, G. M., 2008, A generalized modified Weibull distribution for lifetime modeling, *Computational Statistics & Data Analysis*, 53(2), 450–462. http://dx.doi.org/10.1016/j.csda.2008.08.023

[4] Chaudhary, A. K., and Kumar, V., 2021, The ArcTan Lomax distribution with properties and applications, *International Journal of Scientific Research in Science, Engineering and Technology*, 4099, 117-125. https://doi.org/10.32628/IJSRSET218117

[5] Chen, Z., 2000, A new two-parameter lifetime distribution with bathtub shape or increasing failure rate function, *Statistics & Probability Letters*, 49(2), 155-161.

[6] Chen, Z., 2000, A new two-parameter lifetime distribution with bathtub shape or increasing failure rate function, *IEEE Transactions on Reliability*, 49(1), 50-55. 10.1109/24.855536

[7] Gelman, A., Carlin, J. B., Stern, H. S., and Rubin, D. B., 1995, *Bayesian data analysis*, Chapman and Hall/CRC.

[8] Gelman, A., Stern, J. B., Carlin, H. S., Stern, D. B., Dunson, Vehtari, A., and Rubin, D. B., 2013, *Bayesian Data Analysis*, Third Edition.

[9] Gemeay, A. M., Moakofi, T., Balogun, O. S., Ozkan, E., and Hossain, M. M., 2025, Analyzing real data by a new heavy-tailed statistical model, *Modern Journal of Statistics*, 1(1), 1-24. https://doi.org/10.64389/mjs.2025.01108

[10] Guida, M., and Pulcini, G., 2011, A continuous-state Markov model for age-and state-dependent degradation processes, *Structural Safety*, 33(6), 354-366. https://doi.org/10.1016/j.strusafe.2011.06.002

[11] Gupta, R. D., and Kundu, D., 1999, Theory and methods: Generalized exponential distributions, *Australian & New Zealand Journal of Statistics*, 41(2), 173-188.

[12] Kalbfleisch, J. D., and Prentice, R. L., 2002 *The statistical analysis of failure time data*. John Wiley & Sons.

[13] Kaplan, E. L., and Meier, P., 1958, Nonparametric estimation from incomplete observations, *Journal of the American Statistical Association*, 53(282), 457–481. http://www.jstor.org/stable/2281868?origin=JSTOR-pdf

[14] Klein, J. P., and Moeschberger, M. L., 2023, Survival Analysis: Techniques for Censored and Truncated Data, *Springer-Verlag, New York*.

[15] Lan, Y., and Leemis, L. M., 2008, The logistic–exponential survival distribution, *Naval Research Logistics (NRL)*, 55(3), 252-264. 10.1002/nav.20279

[16] Lawless, J. F., 2011, *Statistical models and methods for lifetime data*, John Wiley & Sons.

[17] Lee, E. T., and Wang, J., 2003, S*tatistical methods for survival data analysis*, John Wiley & Sons, ISBN 9780471476299.

[18] Lee Y., 2025, Markov Chain Modeling of Mixed Traffic with Autonomous Vehicles: Partial Participation in Platooning, *Chiang mai journal of science*, 52(4).

[19] Lemonte, A. J., and Cordeiro, G. M., 2011, An extended Lomax distribution, *Statistics*; 47(4), 800–816. https://doi.org/10.1080/02331888.2011.568119

[20] Lomax, K. S., 1954, Business failures: Another example of the analysis of failure data, *Journal of the American Statistical Association*, 49, 847–852. https://doi.org/10.1080/01621459.1954.10501239

[21] Mahmoudi, E., and Jafari, A. A., 2017, The compound class of linear failure rate-power series distributions: Model, properties, and applications, *Communications in Statistics-Simulation and Computation*, 46(2), 1414-1440. https://doi.org/10.1080/03610918.2015.1005232

[22] Sarhan, A. M., Apaloo, J., and Kundu, D., 2024, A new bivariate lifetime distribution: properties, estimations and its extension, *Communications in Statistics - Simulation and Computation*, 53(2), 879–896. https://doi.org/10.1080/03610918.2022.2034866

[23] Smith, R. M., and Bain, L. J., 1975, An exponential power life-testing distribution, Communications in Statistics Theory and Methods, 4(5), 469-481. https://doi.org/10.1080/03610927508827263

[24] Tarvirdizade, B., and Ahmadpour, M., 2025, Unit-Chen distribution and its quantile regression model with applications, *Scientific African*, 27, e02555. https://doi.org/10.1016/j.sciaf.2025.e02555

[25] Telee, L. B. S., and Kumar, V., 2023, Exponentiated Inverse Chen distribution: Properties and applications, *Journal of Nepalese Management Academia*, 1(1), 53-62. https://doi.org/10.3126/jnma.v1i1.62033

[26] Telee, L. B. S., 2025, Bayesian Estimation and MCMC-Based Analysis of the Inverse Exponentiated Exponential Poisson Distribution, *Baneshwor Campus Journal of Academia*, 4, 67-79. https://doi.org/10.3126/bcja.v4i1.90133

[27] Weibull, W., 1951, A statistical distribution function of wide applicability, *Journal of applied mechanics*. https://hal.science/hal-03112318v1